Supporting Information

Crystal reorientation in methylammonium lead iodide perovskite thin film with thermal annealing

Shalinee Kavadiya[1,2], Joseph Strzalka[3], Dariusz M. Niedzwiedzki[4], Pratim Biswas[1,*]

[1] Aerosol and Air Quality Research Laboratory
Department of Energy, Environmental and Chemical Engineering
Washington University in St. Louis, 63130, USA

[2] School of Electrical, Computer, and Energy Engineering
Arizona State University (ASU), Tempe, Arizona 85287-5706, USA

[3] X-ray Science Division
Advanced Photon Source
Argonne National Laboratory, Lemont, USA

[4] Department of Energy, Environmental and Chemical Engineering
Center for Solar Energy and Energy Storage,
Washington University in St. Louis, 63130, USA

* Corresponding author
Email address: pbiswas@wustl.edu
Tel: +1-314-935-5548 Fax: +1-314-935-5464

Experimental Section

The thorough experimental plan with each varied parameters is presented in Table S1 (supporting information). Here we present a discussion on film synthesis and characterization methodologies used.

Film Synthesis

Methylammonium iodide, was purchased from Dyesol, Australia, and lead iodide was purchased from Alfa Aesar, USA. TEC 7 FTO glass substrates were cleaned with soap and water, followed by sonication in acetone and isopropyl alcohol (IPA) (Sigma-Aldrich, USA) for 10 min each. Substrates were further cleaned in UV-ozone cleaner to remove organic impurities. To mimic the solar cell architecture, the perovskite layer was deposited on the TiO_2 electron transporting layer. Firstly, a dense layer of TiO_2 was deposited on the cleaned FTO substrates by spin coating a solution of titanium diisopropoxidebis(acetyl-acetone) (75 wt% in IPA, Sigma-Aldrich, USA), (0.15 M) in *n*-butanol (99.8%, Sigma-Aldrich, USA), and then dried at 125 °C for 5 min. Following that, a mesoporous TiO_2 layer was deposited by spin coating TiO_2 paste (0.12 mg ml^{-1} in ethanol using a 22 nm 16 wt% TiO_2 colloidal paste, Sigma Aldrich, USA) at 5000 rpm for 30 seconds, then annealed at 500 °C for 30 min. The substrates were kept at 50 °C before being spin-coated with the PbI_2 (Alfa Aesar, USA) solution. PbI_2 solution (498 mg ml^{-1} in dimethyl-formamide) was kept at 60 °C and spin coated on the substrates at 5000 rpm. The films were dried at 50 °C for 3 min and 100 °C for 5 min. After cooling the PbI_2-coated substrate to room temperature, the organic precursor, MAI solution in IPA, was electrosprayed. Details of the electrospray deposition are described somewhere else[8]. Values of the electrospray deposition parameters such as voltage applied is 6 kV, substrate-to-needle distance is 3.68 cm, and flow rate is 1 μLPM. The entire fabrication was performed at ambient conditions (no glove box). This

perovskite film was used for all the characterizations before and after annealing. For rapid annealing, the samples were kept on a thermal stage already at 100 °C, annealed for 5 min, and removed quickly from the stage. For slow annealing to perform *in-situ* measurements, the samples were kept on a thermal stage, the temperature was ramped at 20 °C/min rate from 30 °C to reach 100 °C, and cooled slowly at the same rate to reach back to 30 °C.

Characterization

The absorption spectrum of the perovskite film was measured over 400-800 nm using a UV-vis spectrophotometer (UV-2600, Shimadzu, USA) with an integrating sphere (ISR-2600 Plus, Shimadzu, USA). Crystal structure information was obtained using an X-ray diffractometer (XRD, Bruker D8 Advance, Bruker, USA) in theta-theta geometry configured with x-ray wavelength a λ = 1.5418 Å (Cu $K\alpha_1$) under an operating condition of 40 kV. The theta-theta geometry ensures the diffracted intensity is recorded strictly as a function of the component of the photon wave vector transfer normal to the sample surface, $q_z = (4\pi/\lambda)\sin\theta$ where θ is the incident (and reflected) angle. XRD spectra were corrected for the background, and then peak fitting was performed in the range 2θ = 13.6–14.4° using Origin Pro software to deconvolute the two nearby peaks corresponding to (002) and (110) orientations. The fraction of grains orientated in each direction is estimated from the fraction of the area under the individual peak. The surface morphology of the perovskite film was characterized by the field emission scanning electron microscope (FESEM, Nova NanoSEM 230).

GIWAXS was conducted at Beamline 8-ID-E of the Advanced Photon Source, Argonne National Laboratory, with a monochromatic X-ray of energy 10.9 keV[34]. For in-situ measurement, samples were kept on a thermal stage for slow annealing (including temperature ramp up and ramp

down) and GIWAXS patterns were collected at every 5 °C interval. The X-ray beam was defined by slits to be 20 μm vertically and 200 μm horizontally in size and was incident on the samples at an angle of 0.1°, and scattered x-rays were detected using a Pilatus 1M detector (Dectris) at a distance of 0.228 ± 0.001 m from the sample. In order to account for thermal expansion of the stage as well as the substrate material, a test sample was realigned to the incident X-ray at each 5° increment in the temperature. The resulting calibration curve of Z-position vs. temperature for both the temperature ramp up and ramp down span was used to position subsequent samples during measurements. GIWAXS provides two-dimensional patterns of intensity (I) vs. the photon wave vector transfer (q_y, q_z), which were then analyzed using a Matlab based software, GIXSGUI[35]. An azimuthal averaging of each 2D pattern was performed to get a one-dimensional curve of I vs. q ($q = (q_x^2 + q_y^2 + q_z^2)^{1/2}$) at different temperatures.

Table S1. Experimental plan of the study carried out to investigate the effect of annealing on the crystal orientation and finally on the perovskite film properties.

	Annealing temperature (°C)	Time (min)	Substrate temperature during deposition (°C)	Annealing procedure
1. Effect of annealing on the crystal structure	100	5	RT	Rapid annealing
2. Emergence of the two orientation	100	5	RT	Rapid annealing
3. Effect of substrate temperature	100	5	RT 33 40 47 55	Rapid annealing
4. Effect of annealing temperature	40 55 70 85 100	5	RT	Rapid annealing
5. Effect of annealing procedure	100	5	RT	Rapid annealing
	30 to 100	20 K/min rate	RT	Slow annealing
6. Effect of crystal orientation on perovskite film properties	100	5	RT	Rapid annealing

RT: room temperature

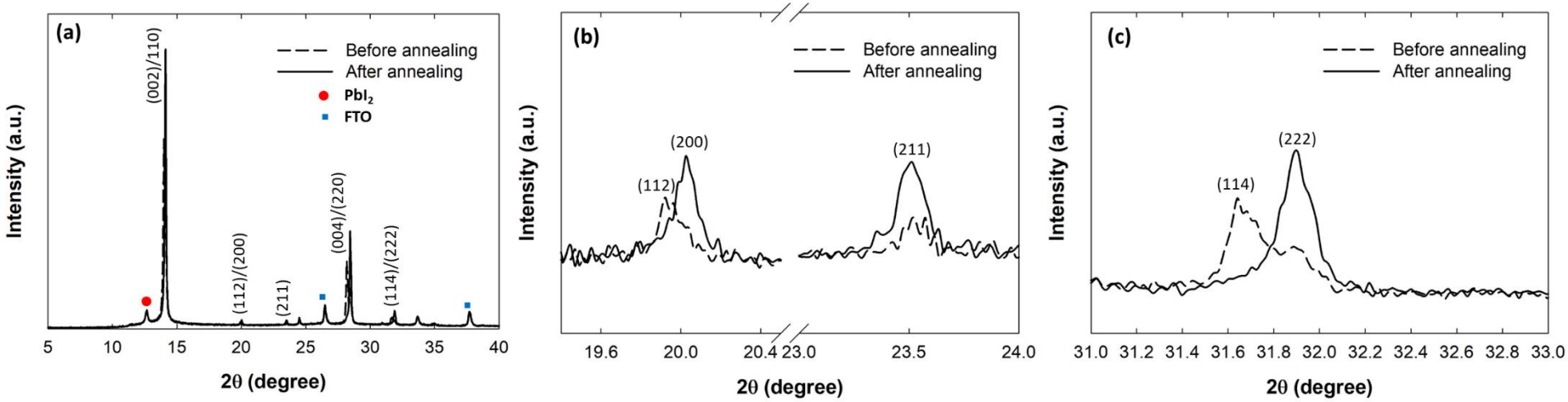

Figure S1. XRD pattern of the electrosprayed perovskite film (same as in Figure 1 in main text) before annealing (dashed curve) and after annealing (solid curve) showing change in (a) (112) and (200) peaks and (b) (114) and (222) peaks with annealing.

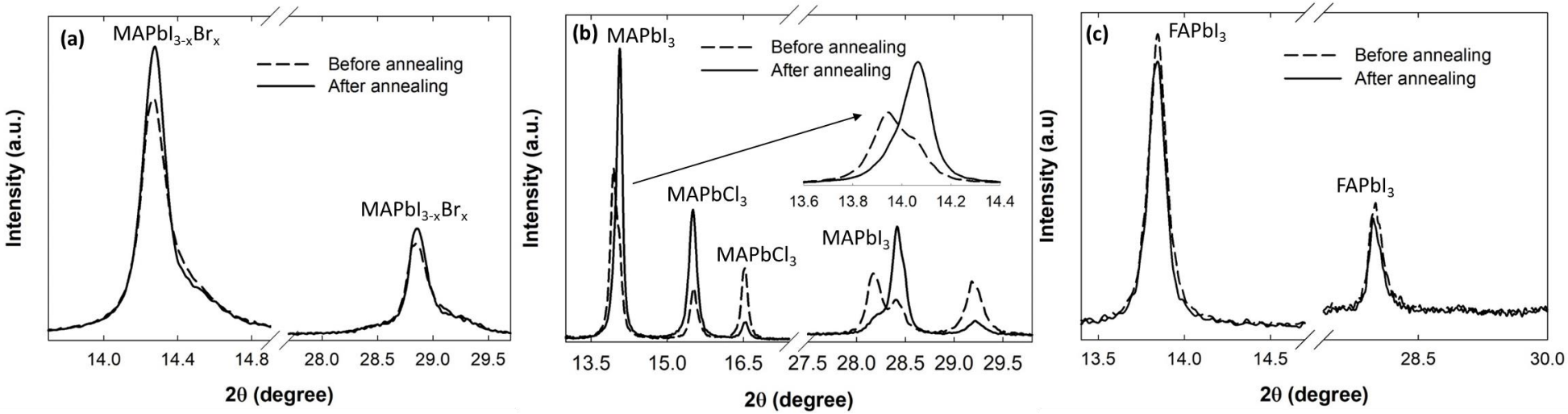

Figure S2. XRD pattern of (a) $MAPbI_{3-x}Br_x$, (b) $MAPbI_{3-x}Cl_x$, and (c) $FAPbI_3$

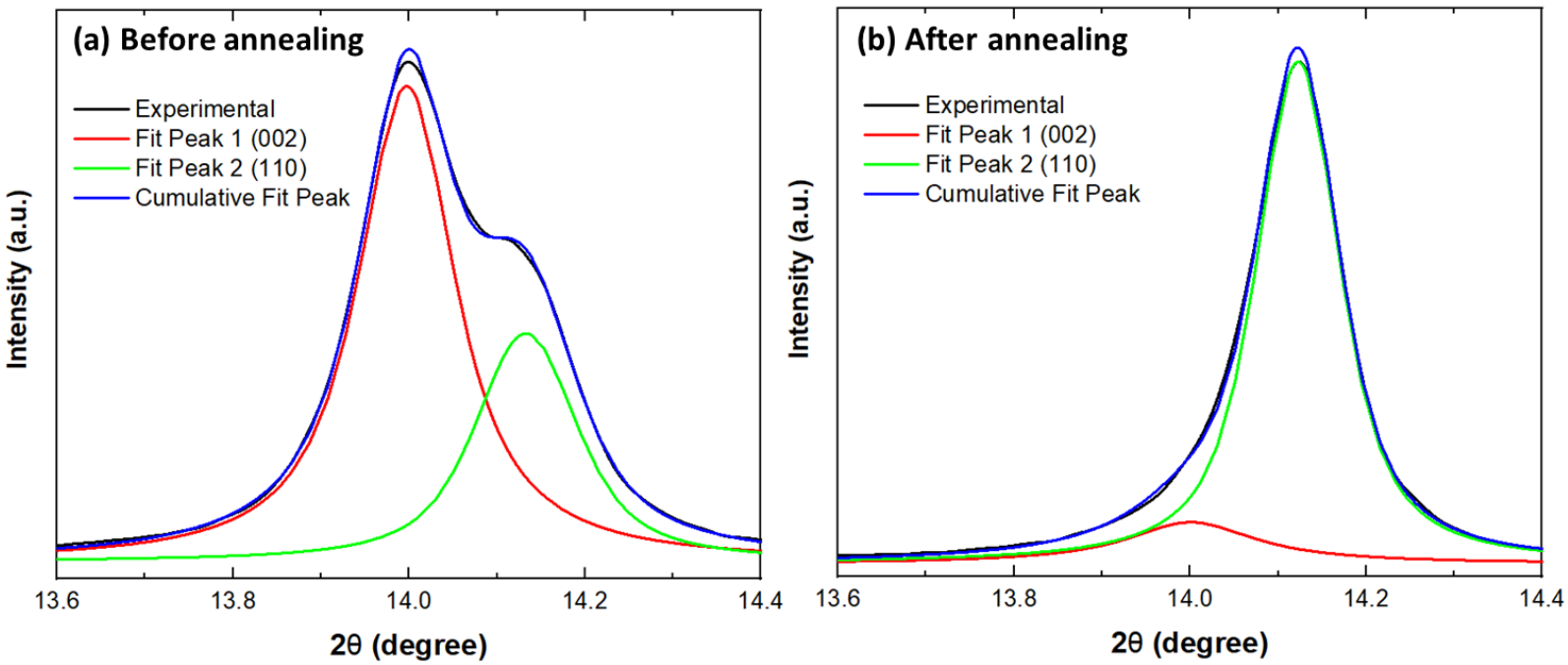

Figure S3. Reconstruction of the XRD spectrum of the perovskite film (a) before and (b) after annealing with sum of two Voigt functions.

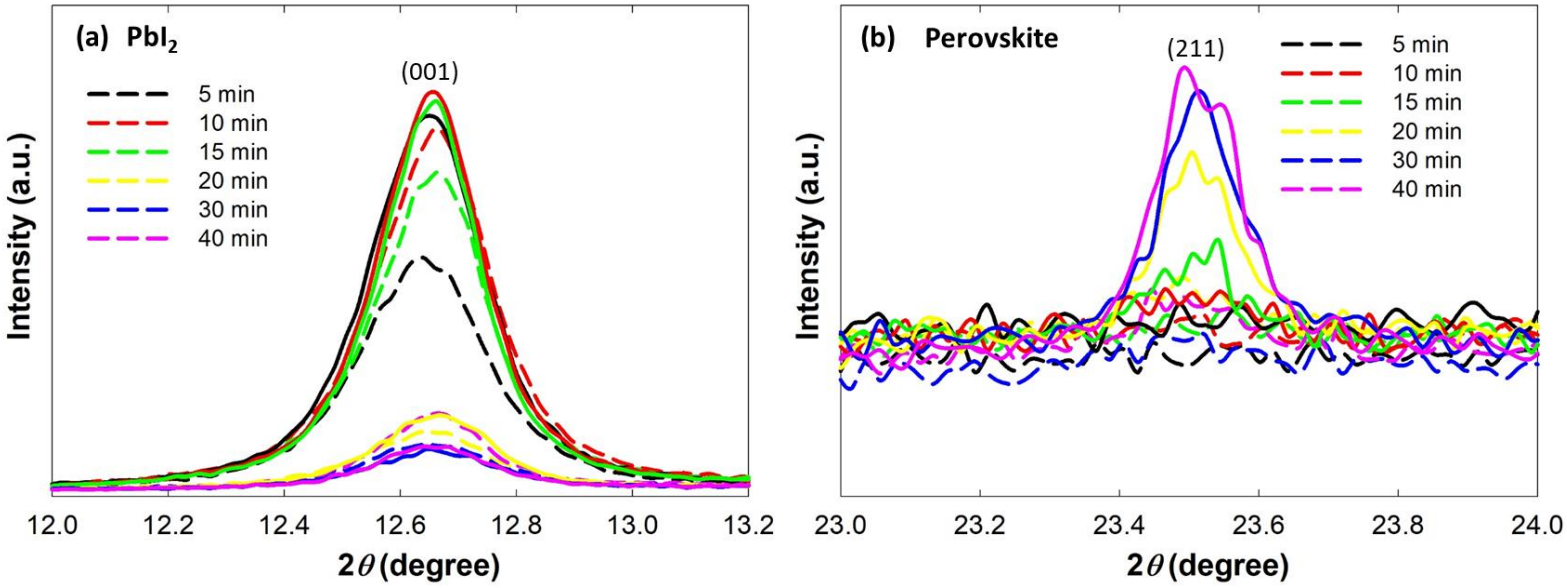

Figure S4. XRD pattern of the perovskite film prepared at different deposition times and taken before annealing (dashed curve) and after annealing (solid curve) focusing (a) PbI_2 (001) peak and (b) perovskite (211) peak.

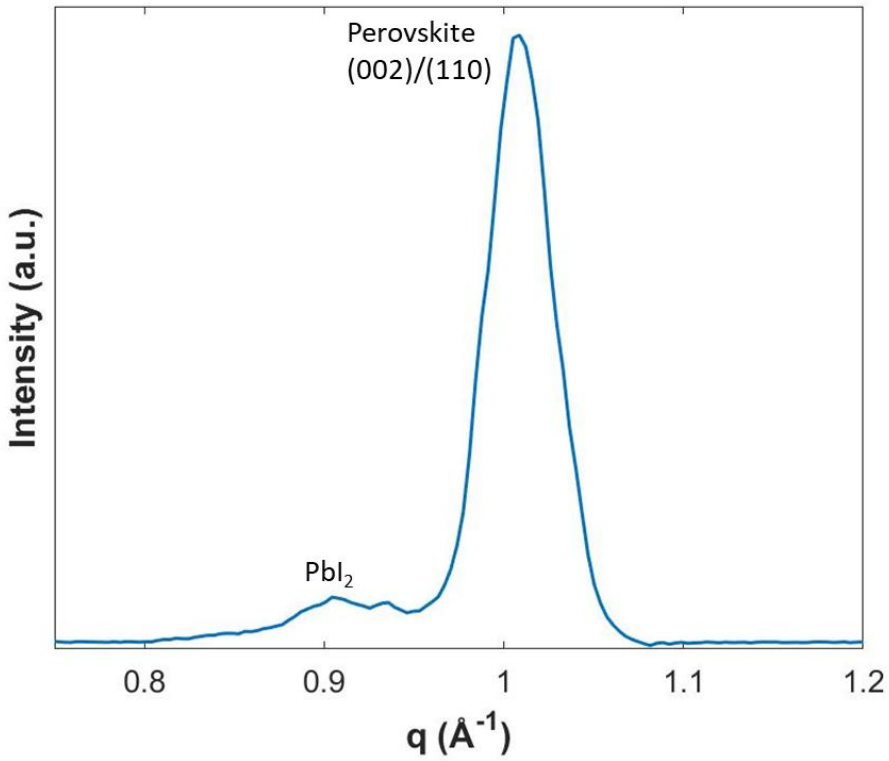

Figure S5. Azimuthal integrated intensity of GIWAXS pattern of the $MAPbI_3$ perovskite before annealing

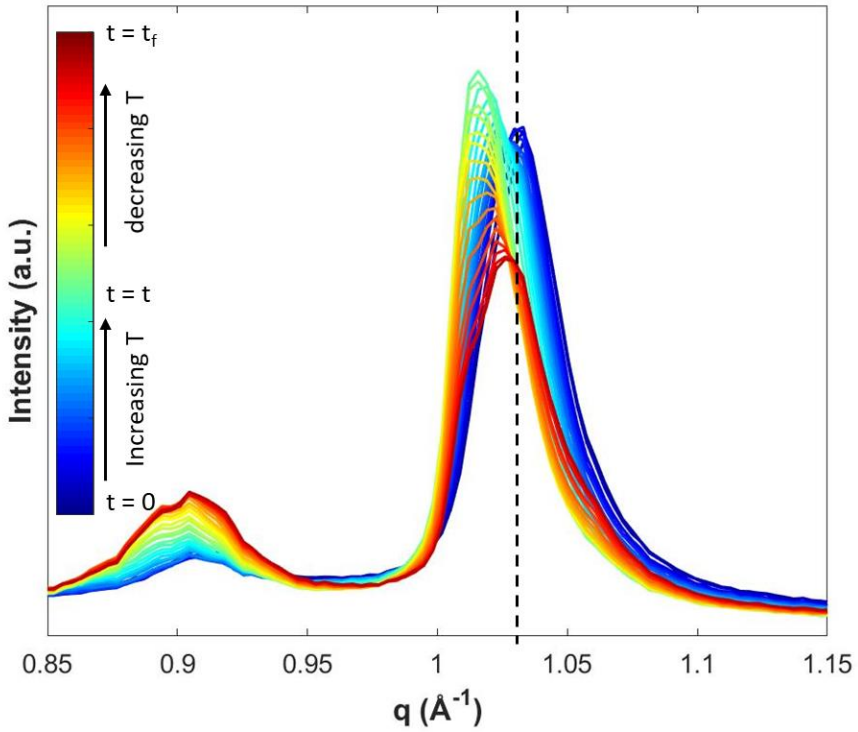

Figure S6. Azimuthal integrated intensity of the GIWAXS pattern of the $MAPbI_{3-x}Br_x$ perovskite film deposited on the TiO_2/FTO substrate as a function of scattering wave vector at different temperature (T) during slow annealing including temperature increase (from t = 0 to t, T = 30 °C to 100 °C) and decrease period (from t = t to t = t_f, T = 100 °C to T = 30 °C).